**CAV2021**
11th International Symposium on Cavitation
May 10-13, 2021, Daejon, Korea

# A volume-of-fluid (VOF) methodology for the prediction of cavitation phenomena

Ali Fakhreddine [1], Karim Alamé [2] and Krishnan Mahesh [2*]

[1]Department of Aerospace Engineering and Mechanics, University of Minnesota, MN 55455, USA
[2]Department of Aerospace Engineering and Mechanics, University of Minnesota, MN 55455, USA

**Abstract:** A sharp interface approach for modeling cavitation phenomena in incompressible viscous flows is presented. We utilize the incompressible Navier-Stokes equations with a modified Poisson equation. The modification to the Poisson equation accounts for phase change taking place at the phase boundary. We adopt a one-fluid formulation for the liquid-vapor two-phase flow and the interface is tracked using a modified volume-of-fluid (VOF) methodology. The modification to VOF is at the level of the advection step whereby the interface is advected with two velocity components, the first one originating from the incompressible flow field, and the second emerging as a result of phase change. The phase change model is extended to account for multiple bubbles via a tagging procedure. The original model and its extension are validated and compared through a Rayleigh-Plesset (RP) bubble collapse.

**Keywords:** cavitation; incompressible flow; volume-of-fluid; bubble tagging

## 1. Introduction

Cavitation is the term used to describe the phase transition of a fluid from liquid to vapor in regions of significant pressure drop. It is observed in vortex cores, turbulent shear flows, and marine propeller applications. Although cavitation can be useful under certain circumstances such as lithotripsy, it is highly undesirable in applications involving lifting surfaces as it is a source of instability and noise. There is complexity associated in the simplest of cavitating flows. This is evident when looking at free-surface and contact line dynamics and studying inception and the mechanisms that sustain cavitation. Ram et. al [1] examined the mechanisms that sustain the inception of attached cavitation. They have found that under certain flow conditions, namely the presence of low momentum zones, microbubbles originating from a collapsed cavity can slowly migrate upstream for a few milliseconds where they either become nuclei for new attached cavitation events or they are swept downstream. The types of events observed in [1] pose several numerical challenges that are required to model and capture the complicated physics involved.

The numerical simulation of cavitating flows has shown rapid progress in the past two decades, however, there are key challenges to be tackled. The principal challenges in the numerical modeling of cavitating flows include sharp changes in density, existence of a moving boundary, and the requirement of accurate modeling of phase change [2]. Earlier work in cavitation modeling has relied primarily on homogeneous mixture modeling which typically requires a phase change model. Amongst the most common phase change models utilized are those developed in [3-4]. A more involved phase change model was later developed in [5] where the effect of non-condensable gas within the vapor cavities was incorporated. The models in [3-4-5] are all based on semi-analytical equations. Other cavitation models are based on a simplification of the classical Rayleigh-Plesset (RP) equation [6-7]. In this work, the focus will be on the development of a numerical method utilizing the latter models [6-7].

Given the presence of a moving boundary in free-surface and multiphase flows, it is common to observe undesirable interface diffusion due to advection, therefore, using a sharp interface computational method to advect the interface is required. Mass conservation, the ability to compute vigorous interface deformation, and the ability to capture topology changes due to break-up and coalescence are collectively

* Corresponding Author: Krishnan Mahesh, kmahesh@umn.edu

desirable features in the simulation of multiphase flows [8]. The volume-of-fluid (VOF) [9], an interface capturing method, has the intrinsic capability of capturing interfacial topology changes directly and can conserve mass exactly given an adequate advection scheme. This method will be utilized in our model for fluid advection.

The objective of this paper is the development of a numerical method based on the incompressible Navier-Stokes equations, that is capable of simulating cavitation phenomena via the addition of a phase change model that is consistent with a sharp interface method. A unique, VOF-based advection scheme is used to move the phase boundary in the presence of phase change. The phase change model is extended to multiple cavities using a Lagrangian tagging procedure following the algorithm in [10]. Finally, we validate the method by simulating a single bubble collapse and the results are compared to the solution of the Rayleigh-Plesset (RP) equation.

## 2. Materials and Methods

Assuming that the liquid and the vapor phase are incompressible and mono-component, and that thermal effects are negligible, the Navier-Stokes equations for incompressible viscous flow are written as:

$$\rho\left(\frac{\partial \boldsymbol{u}}{\partial t}+(\boldsymbol{u}.\nabla)\boldsymbol{u}\right)=-\nabla p+\nabla.\left(\mu(\nabla \boldsymbol{u}+\nabla \boldsymbol{u}^{T})\right)+\boldsymbol{F_{st}}+\delta(n)\boldsymbol{K_{body}} \quad and \quad \nabla.\boldsymbol{u}=0 \tag{1}$$

where $\boldsymbol{\rho}$ denotes density, $\boldsymbol{u}$ is the velocity vector, $\boldsymbol{p}$ denotes pressure, $\boldsymbol{\mu}$ is the dynamic viscosity, $\boldsymbol{F_{st}}$ is the surface tension force, $\boldsymbol{\delta(n)}$ is the Dirac delta function, and $\boldsymbol{K_{body}}$ is the body force which is only active in the liquid phase. We utilize the finite volume algorithm developed in [11] for solving the incompressible Navier-Stokes equations on unstructured grids.

A mass-conserving volume-of-fluid (VOF) methodology is used to track the liquid-vapor interface. The volume fraction is represented by a color function $c$ that varies between a constant value of 1 in a liquid cell to 0 in a vapor cell, with an intermediate value between 0 and 1 to define the phase boundary. The volume of each fluid cell is tracked in a two-step process for each time iteration, reconstruction then advection; the reconstruction and advection steps are based on the analytic relations described in [12]. Given the volume fraction in each cell, the reconstruction of the interface shape uses the local normal vector and a piecewise linear interface calculation (PLIC) to approximate the shape of the interface. The color function $c$ is then advected with the fluid velocity field using a directionally split flux scheme. The scalar transport equation which governs the color function $c$ is given by $\frac{\partial c}{\partial t}+\boldsymbol{u}.\nabla c=0$. Further details on VOF implementation and validation can be found in [13-14-15].

In the presence of phase change, the standard VOF method described above needs to be modified. Phase change implies the addition of an interfacial velocity to the incompressible flow field velocity such that $\boldsymbol{u}=\boldsymbol{u_f}+\boldsymbol{u_{pc}}$ where $\boldsymbol{u}$ is the total fluid velocity, $\boldsymbol{u_f}$ is the incompressible flow field velocity, and $\boldsymbol{u_{pc}}$ is the velocity due to phase change. Starting from the Rankine-Hugoniot jump condition at a phase boundary, we can derive an expression for the total normal interfacial velocity such that $u_\Gamma=\underbrace{\frac{1}{2}(u_v+u_l)}_{u_{\Gamma,\mathrm{f}}}-\underbrace{\frac{\dot{m}}{2}\left(\frac{1}{\rho_v}+\frac{1}{\rho_l}\right)}_{u_{\Gamma,\mathrm{pc}}}$, where $\Gamma$ denotes the interface, $v$ denotes vapor, $l$ denotes liquid, and $\dot{m}$ is the mass flux between the two phases per unit volume. Two approaches were followed to determine the ideal advection scheme for the phase change velocity in order to maintain interface sharpness. In the first approach, the color function is updated using the phase change velocity as a source term such that $\frac{\partial c}{\partial t}=-\frac{\dot{m}}{2}\left(\frac{1}{\rho_v}+\frac{1}{\rho_l}\right)|\nabla c|$. In the second approach, the color function is updated based on the calculated face normals (i.e., sweeping technique) such that $\frac{\partial c}{\partial t}+\boldsymbol{u_{\Gamma,f}}.\nabla c+\boldsymbol{u_{\Gamma,pc}}.\nabla c=0$ where

* Corresponding Author: Krishnan Mahesh, kmahesh@umn.edu

$$\boldsymbol{u}_{\Gamma,\mathrm{pc}} = \begin{cases} u_{\Gamma,\mathrm{pc,x}} = -\dfrac{\dot{m}}{2}\left(\dfrac{1}{\rho_v}+\dfrac{1}{\rho_l}\right)\dfrac{\partial c}{\partial x}\dfrac{1}{|\nabla c|} \\ u_{\Gamma,\mathrm{pc,y}} = -\dfrac{\dot{m}}{2}\left(\dfrac{1}{\rho_v}+\dfrac{1}{\rho_l}\right)\dfrac{\partial c}{\partial y}\dfrac{1}{|\nabla c|} \\ u_{\Gamma,\mathrm{pc,z}} = -\dfrac{\dot{m}}{2}\left(\dfrac{1}{\rho_v}+\dfrac{1}{\rho_l}\right)\dfrac{\partial c}{\partial z}\dfrac{1}{|\nabla c|} \end{cases} \tag{2}$$

In the presence of phase change, a volumetric source term is required due to the difference in density across the interface. The source term is only active at the interface between the two phases; hence the divergence of the velocity field becomes $\nabla.\boldsymbol{u} = \underbrace{0}_{\nabla.\boldsymbol{u_f}} + \underbrace{\dot{m}\left(\frac{1}{\rho_v}-\frac{1}{\rho_l}\right)|\nabla c|}_{\nabla.\boldsymbol{u_{pc}}}$ and the Poisson equation in semi-discrete form becomes $\nabla^2 p^{n+1} = \frac{\rho}{\Delta t}\left(\nabla.\boldsymbol{u_{pc}}\right)^n$.

For an incompressible flow solver that follows a predictor-corrector methodology, the divergence of the velocity field converges to zero such that the velocity field is divergence-free at the end of every time iteration, this however will not be the case at the phase boundary where the volumetric source term is active. Hence, the Poisson equation needs careful treatment since improper discretization of the source term leads to numerical instabilities. In the absence of surface tension, non-condensable gas (NCG), and inertial effects the Rayleigh-Plesset (RP) equation gives $\dot{R}$ such that $\dot{m} = \rho_l \dot{R} = \sqrt{\frac{2\rho_l(p_{vap}-p_\infty)}{3}\left[1-\left(\frac{R_o}{R}\right)^3\right]}$. Because a local pressure will be used instead of a far-field pressure, a correlation factor is needed to correct the mass flux such that $\dot{m} = \alpha_{e,c}\underbrace{\sqrt{p_{vap}-p}}_{to\ be\ linearized}\sqrt{\frac{2}{3}\rho_l\left|1-\left(\frac{R_o}{R}\right)^3\right|}$ where $\alpha_{e,c}$ represents the evaporation and condensation constants, respectively based on the sign of $p_{vap}-p$. Following the linearization in [16], the semi-discrete Poisson equation is finally written as:

$$-\frac{1}{\rho}\nabla^2 p^{n+1} - \underbrace{\frac{1}{\Delta t}\frac{\beta|\nabla c|p^{n+1}}{\sqrt{|p^n - p_{vap}|}}}_{implicit\ term} = \frac{1}{\Delta \mathrm{t}}\left[\nabla.\boldsymbol{u_f^*} - \underbrace{\frac{\beta|\nabla c|p_{vap}}{\sqrt{|p^n - p_{vap}|}}}_{explicit\ term}\right] \tag{3}$$

where $\beta = \alpha_{e,c}\sqrt{\frac{2}{3}\rho_l\left|1-\left(\frac{R_o}{R}\right)^3\right|}\left(\frac{1}{\rho_v}-\frac{1}{\rho_l}\right)$ and $\boldsymbol{u_f^*}$ is the predictor velocity.

The method described uses the color function $c$ to calculate the cavity radius $R$, however since VOF is Eulerian in nature and is incapable of supplying information about each cavity separately, the method will not be useful for a system with multiple cavities. Therefore, we assign a unique identifier id for each separate cavity via a parallel, Lagrangian tagging procedure following [10] and we re-write $\dot{m}$ in terms of cavity volume such that $\dot{m} = \alpha_{e,c}\sqrt{p_{vap}-p}\sqrt{\frac{2}{3}\rho_l\left|1-\left(\frac{V_o}{V}\right)\right|}$. Writing $\dot{m}$ in terms of cavity volume showed better agreement with the RP solution as per the discussion in Section 3.

## 3. Results

### 3.1. Interface advection with phase change

* Corresponding Author: Krishnan Mahesh, kmahesh@umn.edu

Two approaches for interface advection were discussed in Section 2. We choose a constant value of -1 for $\dot{m}$ to initiate bubble collapse on a 256 by 256 uniform grid. Note here that only the scalar transport equation for $c$ is solved.

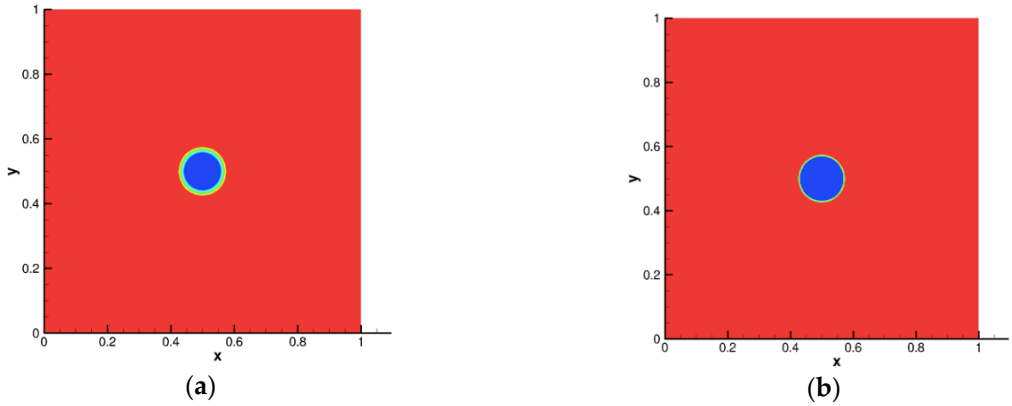


**Figure 1.** Color function contour for an artificial bubble collapse (**a**) using phase change velocity as a source term (**b**) updating the color function based on the calculated normals (sweeping technique)

The results in Figure 1 indicate that advecting the color function $c$ with an additional source term causes undesirable diffusion of the interface while the sweeping technique preserves the sharpness of the interface. The sweeping technique was then utilized to validate the RP bubble collapse. This was done through advecting the color function $c$ via $\dot{R}$ obtained from the RP solution.

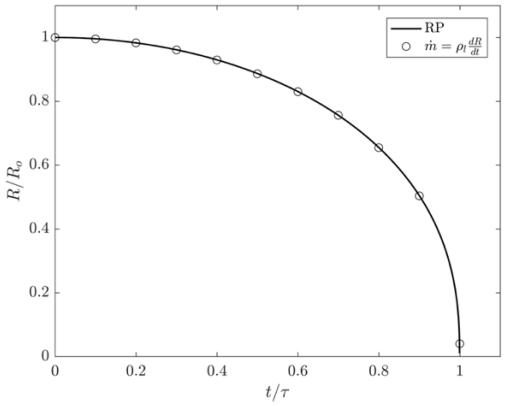


**Figure 2.** Nondimensional radius versus nondimensional time for a single bubble collapse using VOF advection

The advection scheme used recovers the analytic solution.

3.2. Bubble collapse

Computations have been made for a two-dimensional bubble collapse. Given the enforcement of a Dirichlet boundary condition on pressure at the boundaries of the computational domain, it is of interest to investigate the implications of the choice of domain size. Far-field pressure was chosen to be $p_\infty = 100000$ and vapor pressure (pressure inside the bubble) was chosen to be $p_{vap} = 2000$. Bubble radius $R(t)$

* Corresponding Author: Krishnan Mahesh, kmahesh@umn.edu

was nondimensionalized with the initial bubble radius $R_o$ and time t was nondimensionalized with collapse time $\tau$. Figure 3 shows the variation of nondimensional radius with respect to nondimensional time for different domain sizes.

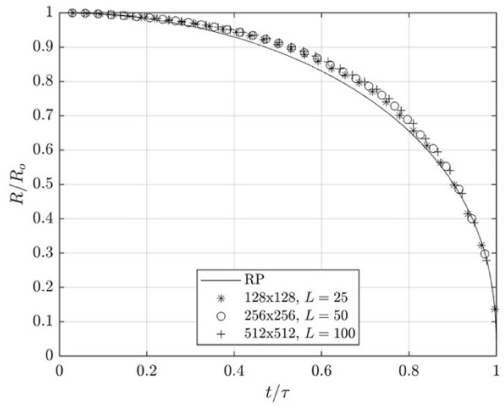


**Figure 3.** Nondimensional radius versus nondimensional time for a single bubble collapse showing the effect of domain size.

The numerical results presented in Figure 3 show good agreement with the RP solution. There is no appreciable influence of domain size.

3.3. Bubble tagging

The phase change model was extended to multiple bubbles/cavities via the addition of a parallel tagging procedure. The tagging procedure was validated in 2D and in 3D across multiple processors.

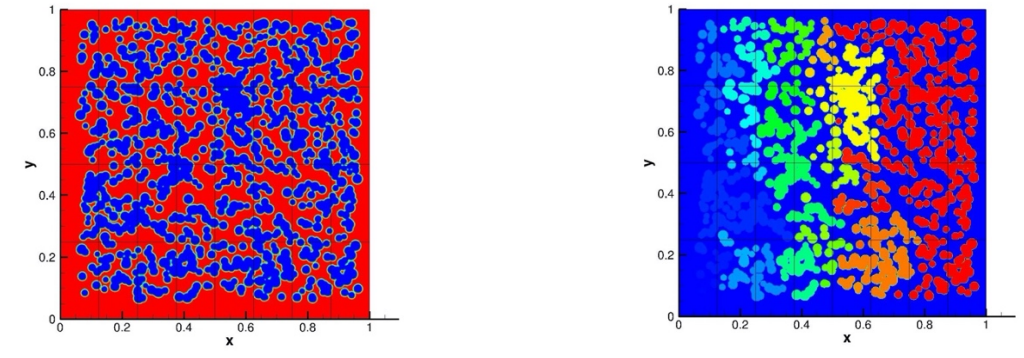


**Figure 4.** Tagging of 1000 bubbles in 2D on multiple processors on a 512 by 512 uniform grid. (**a**) color function contour; and (**b**) tag id contour.

* Corresponding Author: Krishnan Mahesh, kmahesh@umn.edu

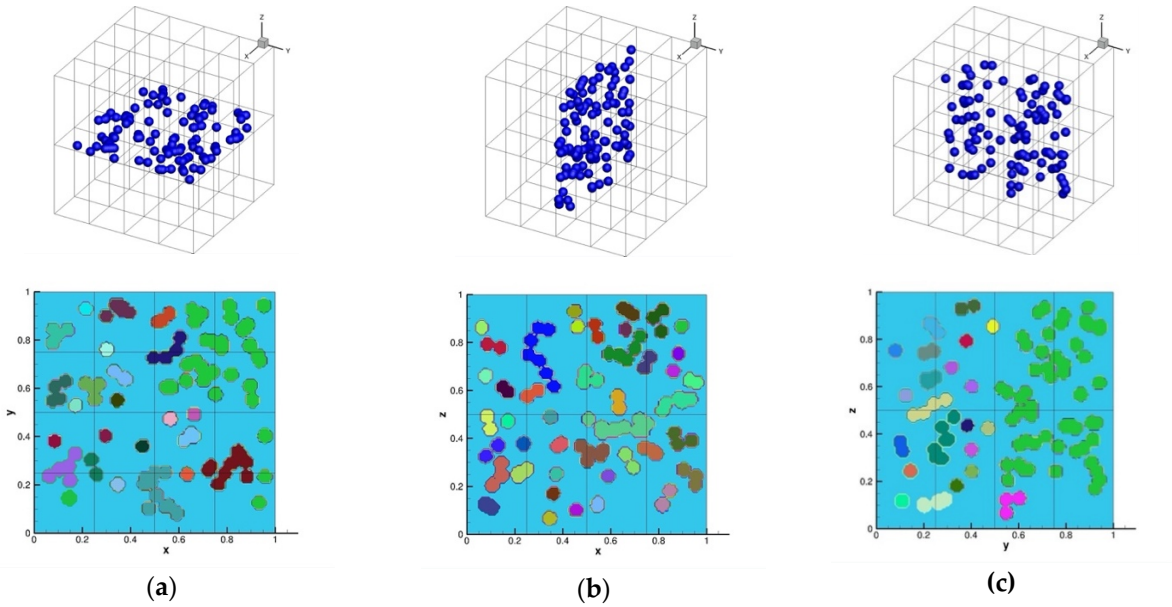


**Figure 5.** Tagging of 70 bubbles on multiple processors in 3D on a 128x128x128 uniform grid. (**a**) tag id contour in x-y plane; (**b**) tag id contour in x-z plane; and (**c**) tag id contour in y-z plane.

### 3.4. Radius formulation vs. Volume formulation

After applying the Lagrangian tagging, the RP collapse problem is simulated using the volume formulation and is compared with the results obtained from the radius formulation. The domain size is $L = 12.5$ and the grid resolution is 128 by 128.

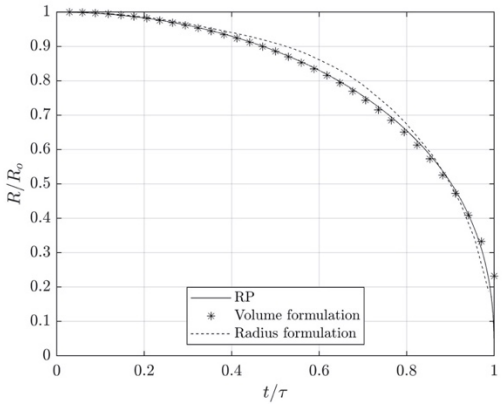


**Figure 6.** Nondimensional radius versus nondimensional time for a single bubble collapse showing a comparison between the radius formulation and volume formulation.

The volume formulation gives more accurate results than the radius formulation as indicated by Figure 6.

## 4. Conclusions

In this work, a sharp interface method for the computation of cavitation phenomena was developed. A phase change model was derived from the Rayleigh-Plesset (RP) equation and extended to

* Corresponding Author: Krishnan Mahesh, kmahesh@umn.edu

simulate multiple cavities via a Lagrangian bubble tagging procedure. The sweeping technique for advection using the phase change velocity was shown to conserve sharpness of the interface. The radius formulation of the phase change model showed good agreement the RP solution for a two-dimensional bubble collapse, however, the volume formulation of the model with bubble tagging presented better agreement. It is foreseen that the phase change model has potential to provide high-fidelity cavitation calculations via the addition of physical effects like gas diffusion and surface tension.

**Acknowledgments:** This work was supported by the United States office of Naval Research (ONR) MURI (Multidisciplinary University Research Initiatives) program under Grant N00014-17-1-2676 with Dr. Ki-Han Kim as the program manager. Computing resources were provided by the Minnesota Supercomputing Institute (MSI).

**References**

1. Ram, O.; Agarwal, K.; Katz, J. On the mechanisms that sustain the inception of attached cavitation. *J. Fluid Mech.* **2020**, 901.
2. Roohi, E.; Zahiri, A.P.; Passandideh-Fard, M. Numerical simulation of cavitation around a two-dimensional hydrofoil using VOF method and the LES turbulence model. *Applied Mathematical Modelling* **2013**, 37, 6569-6488.
3. Merkle, C.L.; Feng, J.Z.; Buelow, P.E.O. Computational modeling of the dynamics of sheet cavitation [C]. *Third International Symposium on Cavitation* **1998**.
4. Kunz, R.F.; Boger, D.A.; Chyczweski, T.S. et al. Multiphase CFD analysis of natural and ventilated cavitation about submerged bodies [C]. *Proceedings of FEDSM '99, 3rd ASME/JSME Joint Fluids Engineering Conference* **1999**.
5. Singhal, A.K.; Athavale, M.M.; Li, H. et al. Mathematical basis and validation of the full cavitation model [J]. *Journal of Fluids Engineering* **2002**, 124(3), 617-624.
6. Sauer, J. Instationaren kaviterendeStroming – Ein neues Modell, baserend auf Front Capturing (VoF) and Blasendynamik. Ph.D. Thesis, Universität, Karlsruhe, 1998.
7. Yuan, W.; Sauer, J.; Schnerr, G.H. Modelling and computation of unsteady cavitation flows in injection nozzles. *J. Mech. Ind.* **2001**, 2, 383-394.
8. Dodd, M.S. Direct numerical simulation of droplet-laden isotropic turbulence. Ph.D. Thesis, University of Washington, 2017.
9. Lafaurie, B.; Nardone, C.; Scardovelli, R.; Zaleski, S.; Zanetti, G. Modelling Merging and Fragmentation in Multiphase Flows with SURFER. *Journal of Computational Physics* **1994**, 113(1), 134-147.
10. Herrmann, M. A parallel Eulerian interface tracking/Lagrangian point particle multi-scale coupling procedure. *Journal of Computational Physics* **2010**, 229(3), 745-759.
11. Mahesh, K.; Constantinescu, G.; Moin, P. A numerical method for large-eddy simulation in complex geometries. *Journal of Computational Physics* **2004**, 197(1), 215-240.
12. Scardovelli, R.; Zaleski, S. Analytical relations connecting linear interfaces and volume fractions in rectangular grids. *Journal of Computational Physics* **2000**, 164(1), 228-237.
13. Alamé, K. Numerical prediction of drag reduction and interfacial shapes over superhydrophobic surfaces. Ph.D. Thesis, University of Minnesota, 2020.
14. Alamé, K.; Mahesh, K. Wall-bounded flow over realistically rough superhydrophobic surface. *J. Fluid Mech.* **2019**, 873.
15. Li, Y.; Alamé, K.; Mahesh, K. Feature-resolved computational and analytical study of laminar drag reduction by superhydrophobic surfaces. *Phys. Rev. Fluids* **2017**, 2.
16. Michael, T.; A sharp interface approach for cavitation modeling using volume-of-fluid and ghost-fluid methods. *Journal of Hydrodynamics* **2017**, 29(6), 917-925.

* Corresponding Author: Krishnan Mahesh, kmahesh@umn.edu